

## On the Origin and Magnitude of Surface Stresses due to Metal Nanofilms

James Bowen,<sup>1\*</sup> David Cheneler<sup>2</sup>

<sup>1</sup> Department of Engineering and Innovation, The Open University, Walton Hall, Milton Keynes, MK7 6AA, UK

<sup>2</sup> Department of Engineering, Lancaster University, Bailrigg, Lancaster, LA1 4YR, UK

\* To whom correspondence should be addressed

Email: [james.bowen@open.ac.uk](mailto:james.bowen@open.ac.uk)

Telephone: + 44 (0) 1908 655 614

## SUPPORTING INFORMATION

| Section number | Section description  | Page number |
|----------------|--|-------------|
| 1              | Cantilever preparation for TEM analysis of the interface structure                               | 2           |
| 2              | Theoretical consideration of beam vertical deflection under the action of surface shear stresses | 3           |
| 3              | Calculated surface shear stresses due to beam metallization                                      | 8           |
| 4              | Calculated beam deflections due to uniformly distributed loads                                   | 9           |
| 5              | Strain due to heteroepitaxial film growth  | 10          |

## 1. Cantilever preparation for TEM analysis of the interface structure

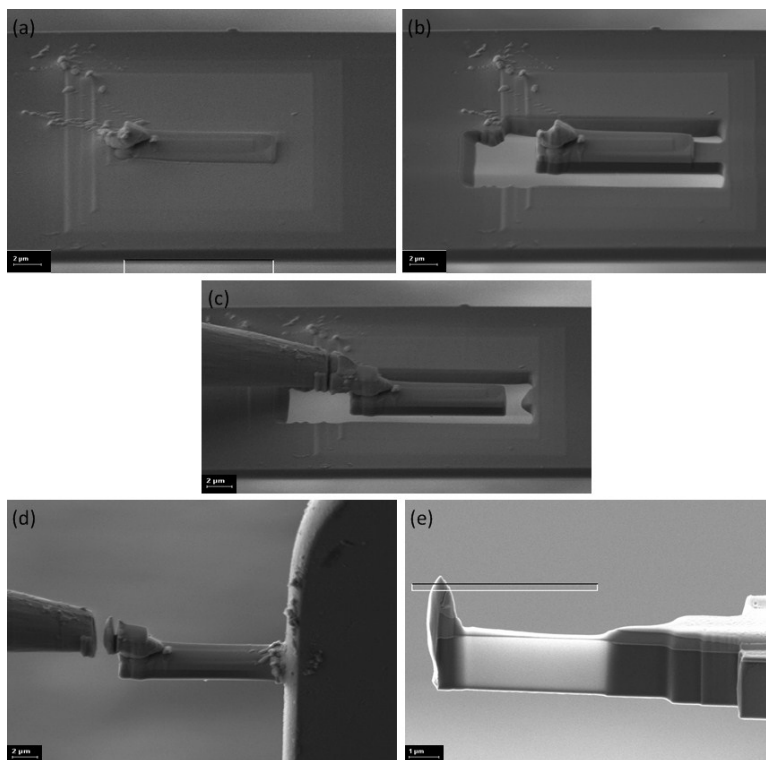


**Figure S1.1** Preparation of the AFM cantilever for TEM analysis.

- (a) Cantilever coated with e-beam sputtered platinum
- (b) Excess material milled out using FIB
- (c) Sample welded to manipulator and milled from cantilever
- (d) Sample welded to TEM stub and milled free from manipulator
- (e) Sample polished sequentially using FIB until *c.a.* 50 nm thick.

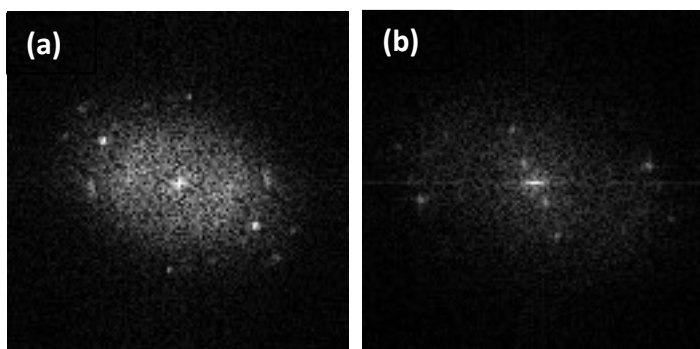


**Figure S1.2** FFT analysis of (a) Ti film and (b) Cr film.

## 2. Theoretical consideration of beam vertical deflection under the action of surface shear stresses

Consider a rectangular beam of length  $L$  and width  $2b$  with a point load  $P$  acting on the end and with a shear stress,  $\tau_1$ , acting on the top surface and another,  $\tau_2$ , acting on the lower surface, as shown in Fig. S2.1:

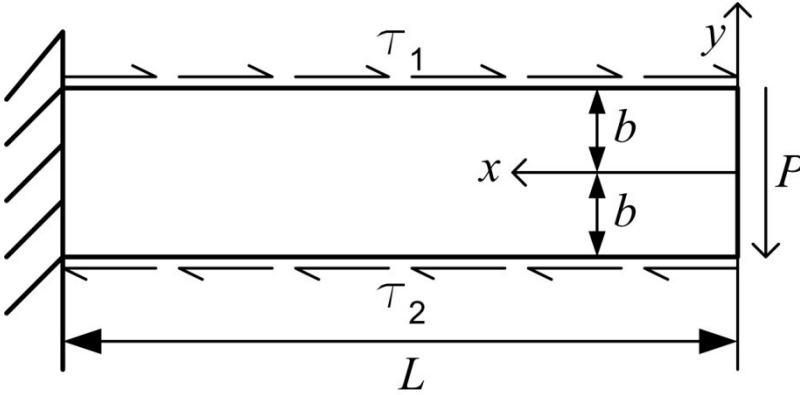


**Figure S2.1** Schematic of a beam under the action of surface shear stresses

In this case the boundary conditions are:

$$\sigma_y = 0, \quad y = \pm b$$

$$\sigma_x = 0, \quad x = 0$$

$$\int_{-b}^b \tau_{xy}(0, y) dy = P', \quad x = 0$$

$$\tau_{xy} = \tau_1, \quad y = b \quad \backslash * \text{MERGEFORMAT (1)}$$

$$\tau_{xy} = \tau_2, \quad y = -b$$

$$\frac{\partial u}{\partial y} = 0, \quad x = L$$

$$u = v = 0, \quad x = L$$

where  $\tau$  and  $\sigma$  denote shear and normal stresses respectively and  $u$  and  $v$  are the axial and vertical displacements.  $P'$  is the force per unit width. To find the stresses within the beam and the resulting displacements, a representative Airy stress function is assumed to exist of the form:

$$\begin{aligned} \phi = & c_1 xy + c_2 x^2 y + c_3 xy^2 + c_4 x^2 y^2 + c_5 x^3 y + c_6 x^3 y^2 + c_7 x^2 + \dots \\ & c_8 y^2 + c_9 x^3 + c_{10} y^3 + c_{11} xy^3 + c_{12} x^2 y^3 + c_{13} x^3 y^3 + c_{14} x^4 + \dots \\ & c_{15} x^4 y + c_{16} x^4 y^2 + c_{17} x^4 y^3 + c_{18} x^4 y^4 + c_{19} y^4 + c_{20} xy^4 + \dots \\ & c_{21} x^2 y^4 + c_{22} x^3 y^4 \end{aligned} \quad \backslash * \text{MERGEFORMAT (2)}$$

where  $c$  denotes an unknown constant. From this the stresses can be directly found to be:

$$\begin{aligned} \sigma_x = \frac{\partial^2 \phi}{\partial y^2} = & 2c_3 x + 2c_4 x^2 + 2c_6 x^3 + 2c_8 + 6c_{10} y + 6c_{11} xy + 6c_{12} x^2 y + 6c_{13} x^3 y + \dots \\ & 2c_{16} x^4 + 6c_{17} x^4 y + 12c_{18} x^4 y^2 + 12c_{19} y^2 + 12c_{20} xy^2 + 12c_{21} x^2 y^2 + 12c_{22} x^3 y^2 \end{aligned} \quad \backslash * \text{MERGEFORMAT (3)}$$

$$\sigma_y = \frac{\partial^2 \phi}{\partial x^2} = 2c_2y + 2c_4y^2 + 6c_5xy + 6c_6xy^2 + 2c_7 + 6c_9x + 2c_{12}y^3 + 6c_{13}xy^3 + \dots \quad \backslash * \text{ MERGEFORMAT (4)}$$

$$12c_{14}x^2 + 12c_{15}x^2y + 12c_{16}x^2y^2 + 12c_{17}x^2y^3 + 12c_{18}x^2y^4 + 2c_{21}y^4 + 6c_{22}xy^4$$

$$\tau_{xy} = -\frac{\partial^2 \phi}{\partial x \partial y} = -c_1 - 2c_2x - 2c_3y - 4c_4xy - 3c_5x^2 - 6c_6x^2y - 3c_{11}y^2 - 6c_{12}xy^2 - \dots \quad \backslash * \text{ MERGEFORMAT}$$

$$6c_{13}x^2y^2 - 4c_{15}x^3 - 8c_{16}x^3y - 12c_{17}x^3y^2 - 16c_{18}x^3y^3 - 4c_{20}y^3 - 8c_{21}xy^3 - 12c_{22}x^2y^3$$

(5)

Employing the boundary conditions given in Eq. 1, the tractions on each surface can be found:

On  $y = b$ :

$$\sigma_y(x, b) = 2c_2b + 2c_4b^2 + 6c_5xb + 6c_6xb^2 + 2c_7 + 6c_9x + 2c_{12}b^3 + 6c_{13}xb^3 + \dots \quad \backslash * \text{ MERGEFORMAT (6)}$$

$$12c_{14}x^2 + 12c_{15}x^2b + 12c_{16}x^2b^2 + 12c_{17}x^2b^3 + 12c_{18}x^2b^4 + 2c_{21}b^4 + 6c_{22}xb^4 = 0$$

$$\tau_{xy}(x, b) = -c_1 - 2c_2x - 2c_3b - 4c_4xb - 3c_5x^2 - 6c_6x^2b - 3c_{11}b^2 - 6c_{12}xb^2 - 6c_{13}x^2b^2 \dots \quad \backslash * \text{ MERGEFORMAT}$$

$$4c_{15}x^3 - 8c_{16}x^3b - 12c_{17}x^3b^2 - 16c_{18}x^3b^3 - 4c_{20}b^3 - 8c_{21}xb^3 - 12c_{22}x^2b^3 = \tau_1$$

(7)

On  $y = -b$ :

$$\sigma_y(x, -b) = -2c_2b + 2c_4b^2 - 6c_5xb + 6c_6xb^2 + 2c_7 + 6c_9x - 2c_{12}b^3 - 6c_{13}xb^3 + \dots \quad \backslash * \text{ MERGEFORMAT (8)}$$

$$12c_{14}x^2 - 12c_{15}x^2b + 12c_{16}x^2b^2 - 12c_{17}x^2b^3 + 12c_{18}x^2b^4 + 2c_{21}b^4 + 6c_{22}xb^4 = 0$$

$$\tau_{xy}(x, -b) = -c_1 - 2c_2x + 2c_3b + 4c_4xb - 3c_5x^2 + 6c_6x^2b - 3c_{11}b^2 - 6c_{12}xb^2 - 6c_{13}x^2b^2 \dots \quad \backslash * \text{ MERGEFORMAT}$$

$$4c_{15}x^3 + 8c_{16}x^3b - 12c_{17}x^3b^2 + 16c_{18}x^3b^3 + 4c_{20}b^3 + 8c_{21}xb^3 + 12c_{22}x^2b^3 = \tau_2$$

(9)

The equilibrium equation and resultant forces become:

$$\frac{\partial^4 \phi}{\partial x^4} + \frac{\partial^4 \phi}{\partial x^2 \partial y^2} + \frac{\partial^4 \phi}{\partial y^4} = 8c_4 + 24c_6x + 24c_{12}y + 72c_{13}xy + 24c_{14} + \dots$$

$$24c_{15}y + 24c_{16}(y^2 + 2x^2) + 24c_{17}y(y^2 + 6x^2) + 24c_{18}(x^4 + 12x^2y^2 + y^4) + \dots \quad \backslash * \text{ MERGEFORMAT (10)}$$

$$24c_{19} + 24c_{20}x + 24c_{21}(x^2 + 2y^2) + 24c_{22}x(x^2 + 6y^2) = 0$$

$$F_x = \int_{-b}^b \sigma_x(0, y) dy = 4c_8b + 8c_{19}b^3 = 0 \quad \backslash * \text{ MERGEFORMAT (11)}$$

$$F_y = \int_{-b}^b \tau_{xy}(0, y) dy = -2c_1b - 2c_{11}b^3 = P' \quad \backslash * \text{ MERGEFORMAT (12)}$$

Equating coefficients and solving Eqs. 3-12 to find the unknown constants gives the Airy stress function as:

$$\phi = -\frac{3P'xy}{4b} + \frac{P'xy^3}{4b^3} + \frac{\tau_1 + \tau_2}{4b^2}xy(b^2 - y^2) + \frac{\tau_2 - \tau_1}{4b}xy^2 \quad \backslash * \text{ MERGEFORMAT (13)}$$

The stress state in the beam can therefore be shown to be:

$$\sigma_x = \frac{3P'xy}{2b^3} - 3\frac{\tau_1 + \tau_2}{2b^2}xy + \frac{\tau_2 - \tau_1}{2b}x \quad \backslash * \text{ MERGEFORMAT (14)}$$

$$\sigma_y = 0 \quad \backslash * \text{ MERGEFORMAT (15)}$$

$$\tau_{xy} = \frac{3P'}{4b^3}(b^2 - y^2) + \frac{\tau_1 + \tau_2}{4b^2}(3y^2 - b^2) - \frac{\tau_2 - \tau_1}{2b}y \quad \backslash * \text{ MERGEFORMAT (16)}$$

The resultant strain field becomes:

$$\varepsilon_x = \frac{3P'xy}{2Eb^3} - 3\frac{\tau_1 + \tau_2}{2Eb^2}xy + \frac{\tau_2 - \tau_1}{2Eb}x = \frac{\partial u}{\partial x} \quad \backslash * \text{ MERGEFORMAT (17)}$$

$$\varepsilon_y = -\frac{3\nu P'xy}{2Eb^3} + 3\nu\frac{\tau_1 + \tau_2}{2Eb^2}xy - \nu\frac{\tau_2 - \tau_1}{2Eb}x = \frac{\partial v}{\partial y} \quad \backslash * \text{ MERGEFORMAT (18)}$$

$$\gamma_{xy} = \frac{3P'}{8Gb^3}(b^2 - y^2) + \frac{\tau_1 + \tau_2}{8Gb^2}(3y^2 - b^2) - \frac{\tau_2 - \tau_1}{4Gb}y = \frac{1}{2}\left(\frac{\partial u}{\partial y} + \frac{\partial v}{\partial x}\right) \quad \backslash * \text{ MERGEFORMAT (19)}$$

where  $E$  is the Young's modulus, and  $G$  is the shear modulus.

Integrating Eqs. 17 and 18 gives:

$$u = \frac{3P'x^2y}{4Eb^3} - 3\frac{\tau_1 + \tau_2}{4Eb^2}x^2y + \frac{\tau_2 - \tau_1}{4Eb}x^2 + f(y) \quad \backslash * \text{ MERGEFORMAT (20)}$$

$$v = -\frac{3\nu P'xy^2}{4Eb^3} + 3\nu\frac{\tau_1 + \tau_2}{4Eb^2}xy^2 - \nu\frac{\tau_2 - \tau_1}{2Eb}xy + g(x) \quad \backslash * \text{ MERGEFORMAT (21)}$$

Substituting these expressions into Eq. 19 gives:

$$\begin{aligned} & \frac{3P'x^2}{8Eb^3} - 3\frac{\tau_1 + \tau_2}{8Eb^2}x^2 + \frac{df(y)}{dy} - \frac{3\nu P'y^2}{8Eb^3} + 3\nu\frac{\tau_1 + \tau_2}{8Eb^2}y^2 - \nu\frac{\tau_2 - \tau_1}{4Eb}y + \frac{dg(x)}{dx} = \dots \\ & \frac{3P'}{8Gb^3}(b^2 - y^2) + \frac{\tau_1 + \tau_2}{8Gb^2}(3y^2 - b^2) - \frac{\tau_2 - \tau_1}{4Gb}y \end{aligned} \quad \backslash * \text{ MERGEFORMAT (22)}$$

Let:

$$A = \frac{3P'x^2}{8Eb^3} - 3\frac{\tau_1 + \tau_2}{8Eb^2}x^2 + \frac{dg(x)}{dx} \quad \backslash * \text{ MERGEFORMAT (23)}$$

$$B = \frac{3P'y^2(2+\nu)}{8Eb^3} - 3(2+\nu)\frac{\tau_1 + \tau_2}{8Eb^2}y^2 + (2+\nu)\frac{\tau_2 - \tau_1}{4Eb}y + \frac{df(y)}{dy} \quad \backslash * \text{ MERGEFORMAT (24)}$$

$$K = \frac{3P'}{8Gb} - \frac{\tau_1 + \tau_2}{8G} \quad \backslash * \text{ MERGEFORMAT (25)}$$

Rearranging and integrating Eqs. 23 and 24 in turn gives:

$$g(x) = -\frac{P'x^3}{8Eb^3} + \frac{\tau_1 + \tau_2}{8Eb^2}x^3 + Ax + C \quad \backslash * \text{ MERGEFORMAT (26)}$$

$$f(y) = -\frac{P'y^3(2+\nu)}{8Eb^3} + (2+\nu)\frac{\tau_1+\tau_2}{8Eb^2}y^3 - (2+\nu)\frac{\tau_2-\tau_1}{8Eb}y^2 + By + D \quad \backslash * \text{ MERGEFORMAT (27)}$$

Substituting Eqs. 26 and 27 into eq. 21 and 20 respectively gives:

$$u = \frac{P'y}{8Eb^3}(6x^2 - y^2(2+\nu)) + \frac{\tau_2-\tau_1}{8Eb}(2x^2 - (2+\nu)y^2) + \dots \quad \backslash * \text{ MERGEFORMAT (28)}$$

$$\frac{\tau_1+\tau_2}{8Eb^2}y((2+\nu)y^2 - 6x^2) + By + D$$

$$v = -\frac{P'x}{8Eb^3}(6\nu y^2 + x^2) + \frac{\tau_1+\tau_2}{8Eb^2}x(6\nu y^2 + x^2) - \nu\frac{\tau_2-\tau_1}{2Eb}xy + Ax + C \quad \backslash * \text{ MERGEFORMAT (29)}$$

where  $A, B, C$  and  $D$  are unknown functions to be found. The boundary conditions  $u(L, 0) = v(L, 0) = 0$  lead to:

$$D = -\frac{\tau_2-\tau_1}{4Eb}L^2 \quad \backslash * \text{ MERGEFORMAT (30)}$$

$$C = \frac{P'L^3}{8Eb^3} - \frac{\tau_1+\tau_2}{8Eb^2}L^3 - AL \quad \backslash * \text{ MERGEFORMAT (31)}$$

The boundary condition  $du/dy(L, 0) = 0$  leads to:

$$B = -\frac{3P'L^2}{4Eb^3} + 3\frac{\tau_1+\tau_2}{4Eb^2}L^2 \quad \backslash * \text{ MERGEFORMAT (32)}$$

Putting these expressions back into Eq. 22 gives:

$$A = \frac{3P'L^2}{4Eb^3} + \frac{3P'}{4Gb} - \frac{\tau_1+\tau_2}{8G} - 3\frac{\tau_1+\tau_2}{4Eb^2}L^2 \quad \backslash * \text{ MERGEFORMAT (33)}$$

Therefore the complete description of the displacements within a stressed beam with a point load is:

$$u = \frac{P'y}{8Eb^3}(6x^2 - y^2(2+\nu) - 6L^2) + \frac{\tau_2-\tau_1}{8Eb}(2x^2 - (2+\nu)y^2 - 2L^2) + \dots \quad \backslash * \text{ MERGEFORMAT (34)}$$

$$\frac{\tau_1+\tau_2}{8Eb^2}y(6L^2 + (2+\nu)y^2 - 6x^2)$$

$$v = \frac{P'}{8Eb^3}(6L^2x - 6\nu xy^2 - x^3 - 4L^3) + \frac{3P'}{4Gb}(x - L) + \dots \quad \backslash * \text{ MERGEFORMAT (35)}$$

$$\frac{\tau_1+\tau_2}{8Eb^2}(-6L^2x + 6\nu xy^2 + x^3 + 4L^3) - \nu\frac{\tau_2-\tau_1}{2Eb}xy - \frac{\tau_1+\tau_2}{8G}(x - L)$$

Or in terms of the second moment of area, defined as:

$$I = \frac{2}{3}wb^3 \quad \backslash * \text{ MERGEFORMAT (36)}$$

where  $w$  denotes the width of the beam:

$$u = \frac{Py}{6EI}(3x^2 - y^2(2+\nu) - 3L^2) + \frac{\tau_2-\tau_1}{12EI}wb^2(2x^2 - (2+\nu)y^2 - 2L^2) + \dots \quad \backslash * \text{ MERGEFORMAT (37)}$$

$$\frac{\tau_1+\tau_2}{6EI}wyb(3L^2 + (2+\nu)y^2 - 3x^2)$$

$$v = \frac{P}{6EI} (3L^2x - 3\nu xy^2 - x^3 - 2L^3) + \frac{Pb^2}{2GI} (x-L) + \dots \quad \backslash * \text{ MERGEFORMAT (38)}$$

$$\frac{\tau_1 + \tau_2}{6EI} wb (-3L^2x + 3\nu xy^2 + x^3 + 2L^3) - \nu \frac{\tau_2 - \tau_1}{2Eb} xy - \frac{\tau_1 + \tau_2}{8G} (x-L)$$

where  $P = P'w$  and is in Newtons.

When  $\tau_1 = \tau_2 = 0$ :

$$u = \frac{Py}{6EI} (3x^2 - y^2 (2 + \nu) - 3L^2) \quad \backslash * \text{ MERGEFORMAT (39)}$$

$$v = \frac{P}{6EI} (3L^2x - 3\nu xy^2 - x^3 - 2L^3) + \frac{Pb^2}{2GI} (x-L) \quad \backslash * \text{ MERGEFORMAT (40)}$$

This is the result given by the analysis of the unstressed beam. As it is only the vertical deflection that is of concern here, it is interesting to consider a few special cases. For instance the shape of the beam due to surface stresses when there is no external load is given by Eq. 41:

$$v = \frac{\tau_1 + \tau_2}{6EI} wb (-3L^2x + 3\nu xy^2 + x^3 + 2L^3) - \nu \frac{\tau_2 - \tau_1}{2Eb} xy - \frac{\tau_1 + \tau_2}{8G} (x-L) \quad \backslash * \text{ MERGEFORMAT (41)}$$

Assuming the beam is thin so that the deflection is that of the centre of the beam, i.e. when  $y = 0$ , the deflection is given as:

$$v = \frac{\tau_1 + \tau_2}{6EI} wb (-3L^2x + x^3 + 2L^3) - \frac{\tau_1 + \tau_2}{8G} (x-L) \quad \backslash * \text{ MERGEFORMAT (42)}$$

Eq. 42 was fitted to the measured interferometric data in order to ascertain the stress on the top surface.  $\tau_2$  was assumed to be 0 as there was no metal deposition on the underside of the beam.

### 3. Calculated surface shear stresses due to beam metallisation

| Cantilever | Beam length, $L$ ( $\mu\text{m}$ ) | Beam width, $w$ ( $\mu\text{m}$ ) | Beam resonant frequency, $\nu$ (kHz) | Beam thickness, $2b$ ( $\mu\text{m}$ ) | Thickness of deposited metal film, $t_f$ (nm) | Initial oxide thickness, $t_{ox}$ (nm) | Initial spring constant, $k$ (N/m) | Upper surface shear stress, $\tau_1$ (kPa) |
|------------|------------------------------------|-----------------------------------|--------------------------------------|--|---|--|------------------------------------|--|
| Ti 01      | 90                                 | 35                                | 200.8                                | 1.24                                   | 4.5   | 3.7                                    | 3.48                               | -12.3                                      |
| Ti 02      | 110                                | 35                                | 124.7                                | 1.15                                   | 4.5   | 3.7                                    | 1.52                               | -10.1                                      |
| Ti 03      | 130                                | 35                                | 87.6                                 | 1.13                                   | 4.5   | 3.7                                    | 0.87                               | -8.5                                       |
| Ti 04      | 90                                 | 35                                | 213.3                                | 1.32                                   | 4.5   | 3.5                                    | 4.17                               | -12.3                                      |
| Ti 05      | 110                                | 35                                | 135.2                                | 1.25                                   | 4.5   | 3.5                                    | 1.94                               | -10.1                                      |
| Ti 06      | 130                                | 35                                | 92.7                                 | 1.20                                   | 4.5   | 3.5                                    | 1.05                               | -8.5                                       |
| Ti 07      | 90                                 | 35                                | 201.7                                | 1.25                                   | 12.0  | 3.9                                    | 3.56                               | -74.7                                      |
| Ti 08      | 110                                | 35                                | 133.9                                | 1.24                                   | 12.0  | 3.9                                    | 1.89                               | -61.1                                      |
| Ti 09      | 130                                | 35                                | 91.6                                 | 1.19                                   | 12.0  | 3.9                                    | 1.02                               | -51.7                                      |
| Ti 10      | 90                                 | 35                                | 196.7                                | 1.22                                   | 12.0  | 3.1                                    | 3.31                               | -74.7                                      |
| Ti 11      | 110                                | 35                                | 132.4                                | 1.23                                   | 12.0  | 3.1                                    | 1.83                               | -61.1                                      |
| Ti 12      | 130                                | 35                                | 91.2                                 | 1.18                                   | 12.0  | 3.1                                    | 0.99                               | -51.7                                      |
| Cr 01      | 90                                 | 35                                | 205.6                                | 1.27                                   | 6.0   | 3.9                                    | 3.74                               | 20.0                                       |
| Cr 02      | 110                                | 35                                | 136.3                                | 1.26                                   | 6.0   | 3.9                                    | 1.94                               | 16.4                                       |
| Cr 03      | 130                                | 35                                | 93.9                                 | 1.21                                   | 6.0   | 3.9                                    | 1.07                               | 13.4                                       |
| Cr 04      | 90                                 | 35                                | 207.9                                | 1.29                                   | 6.0   | 3.3                                    | 3.92                               | 20.0                                       |
| Cr 05      | 110                                | 35                                | 150.7                                | 1.39                                   | 6.0   | 3.3                                    | 2.68                               | 16.4                                       |
| Cr 06      | 130                                | 35                                | 94.4                                 | 1.22                                   | 6.0   | 3.3                                    | 1.10                               | 13.4                                       |
| Cr 07      | 90                                 | 35                                | 187.4                                | 1.16                                   | 12.0  | 3.5                                    | 2.85                               | 143.3                                      |
| Cr 08      | 110                                | 35                                | 129.2                                | 1.20                                   | 12.0  | 3.5                                    | 1.70                               | 117.3                                      |
| Cr 09      | 130                                | 35                                | 88.2                                 | 1.14                                   | 12.0  | 3.5                                    | 0.90                               | 99.2                                       |
| Cr 10      | 90                                 | 35                                | 201.6                                | 1.25                                   | 12.0  | 5.1                                    | 3.56                               | 143.3                                      |
| Cr 11      | 110                                | 35                                | 130.5                                | 1.21                                   | 12.0  | 5.1                                    | 1.75                               | 117.3                                      |
| Cr 12      | 130                                | 35                                | 93.8                                 | 1.21                                   | 12.0  | 5.1                                    | 1.07                               | 99.2                                       |

**Table 1.** Shear stress applied to the upper surface of beams metallised with Ti and Cr, calculated by fitting Eq. 1 to vertical curvature measured using interferometry. Beam thickness and initial spring constant calculated according to the method described Bowen *et al.* [30]



#### 4. Calculated beam deflections due to uniformly distributed loads

The maximum deflection,  $\delta_{max}$ , of a static, nominally horizontal, rectangular cantilever beam under its own weight is given by:

$$\delta_{max} = \frac{mgL^3}{8EI} \quad (43)$$

where,  $m$  = beam mass and is given by Eq. 44,  $g$  = acceleration due to gravity,  $L$  = beam length,  $E$  = Young's modulus, and the second area moment of inertia,  $I$ , is given by Eq. 45.

$$m = Lwt_b\rho_b + Lwt_f\rho_f \quad (44)$$

$$I = \frac{wt^3}{12} \quad (45)$$

Note that  $w$  = beam width,  $t_b$  = beam thickness,  $t_f$  = film thickness,  $\rho_b$  = beam density,  $\rho_f$  = film density.

It is assumed that the film covers the full length and width of the beam upper surface, and that the Young's modulus of the beam is not significantly modified by the presence of the metal film.

Table 2 lists the calculated deflection of the longest cantilevers under consideration in this work, where  $L = 110 \mu\text{m}$ ,  $w = 35 \mu\text{m}$ ,  $g = 9.81 \text{ m/s}^2$ ,  $E = 152 \text{ GPa}$ ,  $t_b = 1 \mu\text{m}$ ,  $\rho_b = 2,130 \text{ kg/m}^3$ .

| Beam      | Metal film thickness (nm) | Metal density (kg/m <sup>3</sup> ) | Beam mass (ng) | Film mass (ng) | Film mass/Beam mass (%) | Maximum beam deflection (pm) |
|-----------|---------------------------|------------------------------------|----------------|----------------|-------------------------|------------------------------|
| No film   | 0                         | -                                  | 8.201          | -              | 0                       | 94.9                         |
| Cr 6 nm   | 6                         | 7,190                              | 8.201          | 0.166          | 2.03                    | 95.8                         |
| Cr 12 nm  | 12                        | 7,190                              | 8.201          | 0.332          | 4.05                    | 97.3                         |
| Ti 4.5 nm | 4.5                       | 4,506                              | 8.201          | 0.078          | 0.95                    | 96.8                         |
| Ti 12 nm  | 12                        | 4,506                              | 8.201          | 0.208          | 2.54                    | 98.7                         |

**Table 2.** Calculated metal film masses and cantilever beam deflections under uniformly distributed load

## 5. Strain due to heteroepitaxial film growth

If the Ti or Cr atoms were sufficiently ordered upon deposition on to the SiO<sub>2</sub> surface, the film growth could be described by a heteroepitaxial model. In such a scenario, the strain could arise from two main sources:

- (i) the difference in the lattice parameter between the metal layer and the substrate, and
- (ii) the difference in the thermal expansion coefficients.

As the film was deposited on an unheated substrate, it is likely that thermal expansion effects can be ignored. The possibility exists therefore that lattice parameter mismatch could be significant. If the lattice parameter difference is accommodated by the elastic deformation of the metal layer, the elastic strain in the metal layer is given by Eq. 46 [32]:

$$\varepsilon \approx \frac{a_m - a_s}{a_s} \quad (46)$$

where  $a_m$  and  $a_s$  are the unstrained lattice parameters of the metal layer and substrate respectively.

It should be noted that for  $a_m > a_s$ , the strain in the metal film is compressive and hence  $\varepsilon$  is positive. Similarly, when  $a_m < a_s$ , the strain in the metal film is tensile and  $\varepsilon$  is negative.

Eq. 46 assumes that only the metal layer is elastically deformed and that there is no strain gradient across the film thickness. In reality, any strain induced in the film will also induce a strain in the substrate, albeit much smaller. These effects are strongly dependent on the thickness of the film.

For the systems investigated in this work, the film thickness is sufficiently small as to make Eq. 46 a reasonable approximation. As the metal film is always in contact with the native SiO<sub>2</sub> layer atop the Si cantilever, the lattice parameter of the substrate is taken to be that of SiO<sub>2</sub>.

| Material                       | Crystal type | Unit cell axis a (Å) | Unit cell axis b (Å) | Unit cell axis c (Å) | Unit cell volume (Å <sup>3</sup> ) | Mean lattice parameter (Å) |
|--------------------------------|--------------|----------------------|----------------------|----------------------|------------------------------------|----------------------------|
| SiO <sub>2</sub>               | Hexagonal    | 4.914                | -                    | 5.405                | 113.03                             | 4.84                       |
| Ti                             | Hexagonal    | 2.95                 | -                    | 4.69                 | 35.32                              | 3.28                       |
| Cr                             | Isometric    | 2.8839               | -                    | -                    | 23.99                              | 2.88                       |
| TiO <sub>2</sub>               | Orthorhombic | 9.1742               | 5.4492               | 5.1382               | 256.87                             | 6.36                       |
| Cr <sub>2</sub> O <sub>3</sub> | Hexagonal    | 4.9607               | -                    | 13.599               | 289.82                             | 6.62                       |

Note: The lattice parameter is an average value found by taking the cube root of the cell volume.

**Table 3.** Unstrained crystal properties of the various materials found deposited onto the cantilevers.

It can be seen from Eq. 46 and Table 3 that the stress in the metal layer would be  $\varepsilon = -0.32$  for Ti and  $\varepsilon = -0.40$  for Cr. This suggests that both Ti and Cr films should both be in tension. However, comparing Figs. 3 and 5, it can be seen that the Cr film has developed a significant Cr<sub>2</sub>O<sub>3</sub> layer, whereas the Ti film did not develop an oxide layer. Cr<sub>2</sub>O<sub>3</sub> has an average lattice parameter larger than both Cr and SiO<sub>2</sub>. Hence it is possible that the Cr<sub>2</sub>O<sub>3</sub> layer could induce a compressive strain, via lattice parameter mismatch. Unfortunately, Eq. 46 does not describe systems with multiple layers of different materials.

While this analysis is standard for analysing epitaxial films, it predicts much larger strains, and therefore stresses, than actually measured. This provides evidence that the films are not deposited epitaxially and that there is likely a significant distribution in the structure and associated local lattice parameters within the metallic film. There is evidence of some long range order and crystallisation in the films, but this seems to be of a granular nature, making a more in-depth analysis of the effects of crystalline orientation akin to that given in [33] inappropriate.